GHz signal quality reception and role of Geomagnetic hazard situation & Equatorial Anomaly: A brief study

M Devi *[1,2], A.K. Barbara[1,2], S Patgiri[3], S Das[3], A Medhi[3], and K.I. Oyama[4,5]

[1]Department of Physics, Gauhati University
[2]Electronic Scientists and Engineers Society, Assam, India
[3]S.T. Radar Centre, Gauhati University
[4]International Center for Space Weather Study and Education, Kyushu University, Fukuoka, Japan
[5]Institute of Plasma and Space Sciences, National Cheng Kung University, Taiwan

Abstract

The association of Equatorial Anomaly with the reception quality of a signal is the scope of this study, by analyzing parameters mainly scintillation, a rapid fluctuation of signal both in amplitude and phase while passing through trans–ionospheric and tropospheric media. The exercise is conducted over periods covering both low (2009-2010) and high solar active status (2015-2016) with the GPS-derived scintillation at 1.2 GHz-1.5 GHz and TEC recorded at Gauhati (26° N,92° E 15° N Geomagnetic latitude), a station over anomaly crest. The scintillation analysis is focused mainly of Post -Sunset hours when the anomaly strength changes at the High and Low Solar Activity status and the role of Geo-Magnetic Storm (GMS) on the "Anomaly induced scintillation" is of particular interest here and thereby on signal reception quality in the environment. Finally, the S4 index strength and temporal occurrence features are associated with ΔTEC_{max} the "maximum magnitude " of TEC fluctuation from the background along with the TEC peak status during the post-sunset anomaly period and examined these parameters as possible contributions to the development/inhibition of scintillation qualified for this period with the emphasis more on GMS environment. The resultant conclusion on signal degradation quality or its improvement is thus coupled with these features of the Anomaly. The primary sources of scintillations are directed to plasma instabilities like Rayleigh Taylor leading to small structure irregularities, the role of lower atmospheric turbulences is also brought into the ambit of discussion. The relevant TEC parameters from the global anomaly crest locations are also presented, as and where necessary.

Keywords : Equatorial Anomaly; Scintillation and signal quality; Geomagnetic Storm; ΔTEC_{max} , TEC_{peak}, Solar Activity

*corresponding author:md555gu@gmail.com

1 Introduction

Before dealing with the main subject matter, a brief background behind the work is presented as an introduction.

1.1 Background

A study on VHF- Scintillation in association with Total Electron Content has been initiated at Gauhati University decades back in 1977 with the installation of an ATS –6 setup receiving the 136 MHz RB signal. The study continued with ETS -2 and then with FLEETSAT and in the analysis process, the seasonal diurnal features on scintillation and solar roles in the growth of small-scale structures leading to scintillation are dealt with [Barman et al., 1993, 2000] and the overall finding was that the scintillation occurrence pattern has high seasonal control over the anomaly location. The present study will be a complemented one to those earlier results with signals entering the microwave range of 1.2 GHz. The L-band scintillations though expected to be low in comparison to the VHF range but have become a vital tool now to study the ionospheric irregularity features along with Total Electron Content (TEC) variations especially during situations like Geomagnetic storms and earthquakes because such study provides inputs for understanding coupling dynamics from the magnetosphere to lower atmosphere [Devi et al., 2018] and also from high to low latitudes, in such hazardous environments.

2 Analysis

The observational results are based on 1.2 GHz a 1.5 GHz scintillation and TEC received from a dual-frequency GPS system with the base station data from Guwahati (26°10′N, 91°45′ E, and 15°N geomagnetic). The analysis covers a period from 2009 to 2016 and as additional inputs, Global TEC profiles are adopted as and when required.
The study period is so selected that it offers a background to examine the growth of scintillation at different solar activity periods spreading from a low solar status to a strong solar (Figure 1) environment. A typical L band Scintillation Index (S4) profile (solstice) presented in Figure. 1, directs that signal reception quality at this frequency may be severely degraded times though a long span of loss of quality may not be expected, however, to evaluate a comprehensive picture of this issue, the role of solar-terrestrial disturbance factors is necessary to evaluate.

We will here mainly analyze the amplitude scintillation index (SI), S_4, a standard index used to measure small-scale disturbances in the atmosphere. It is defined as the ratio of the standard deviation of signal intensity to the average signal intensity [Briggs and Parkin, 1963]. The well-known association between SI and S4 [Whitney, 1974] provides:
SI of $4dB$ to $8dB$ equivalent to $0.2 < S_4 \leq .4$;
$8dB$ to $15dB$ corresponds to $0.4 < S_4 \leq 0.0, 6$ and
$S_4 > 0.6$ signifies $SI \geq 0.6$.

A typical L band Scintillation Index (S_4) profile (solstice) presented in Figure. 2, directs that signal reception quality at this frequency may be severely degraded at times though a long span of loss of quality may not be expected in general. However, to evaluate a comprehensive picture of scintillation growth factors, the contribution of solar-terrestrial disturbance to this phenomenon is necessary.
Added to these aspects, the role of Equatorial anomaly in the scintillation development process still remains a challenging problem and where the paper has the focus, especially when the primary data source is from an anomaly crest station.
The anomaly zone is represented by two peaks of electron density around ±15° geomagnetic latitudes and a trough at the equator. Figure. 3 is a well-known map displaying a variation of geomagnetic latitudes

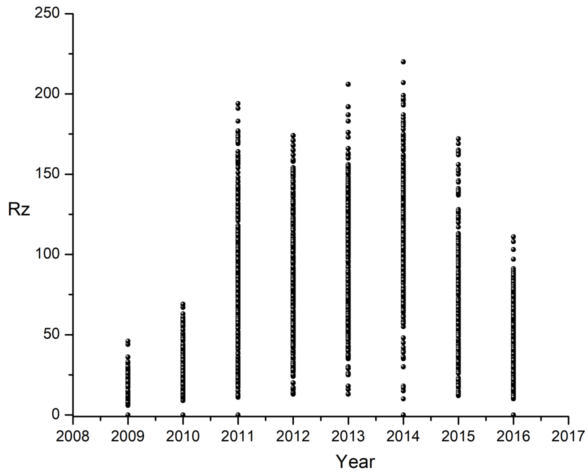

Figure 1: Soar activity status represented by Rz from 2009 to 2016

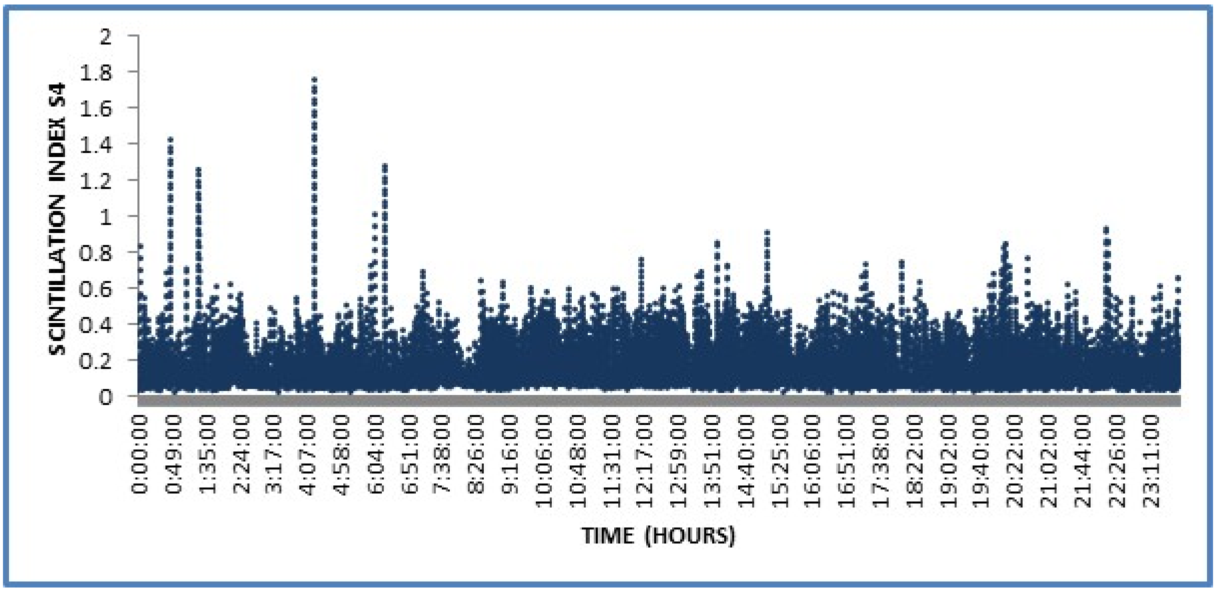

Figure 2: A typical L-Band scintillation index S_4 received by GPS at Guwahati

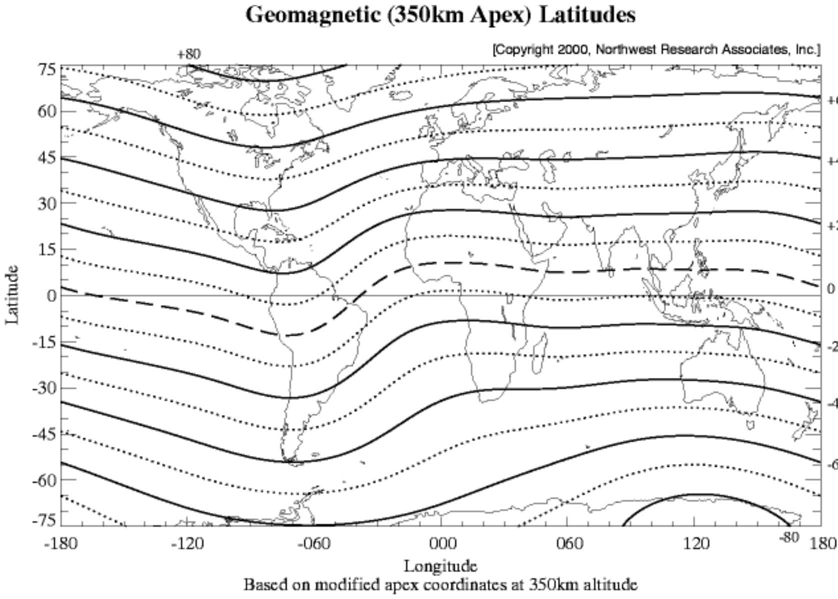

Figure 3: Anomaly belt and geomagnetic latitudes

with longitudes. The ±15° anomaly zone also thus shows a variation with longitudes. This phenomenon along with the Anomaly belt existence as reported decades back [Appleton, 1954] is drawing the attention of ionospheric scientists in understanding ionospheric current and field systems and now its applications get extended to possible use as a hazed predictor. The dumping of plasma from the equator to the low latitude stations through EXB drift process where E is the eastward ionosphere electric field and B is the equatorial earth magnetic field component is identified as the growth process of this phenomenon. The E field during equinoctial months, as is strong, the anomaly is strong during this period. While dealing with scintillation at low-latitude stations this issue is important because anomaly creation and dissipation process are considered as one of the sources of triggering of small-scale structures and may lead to scintillations.

2.1 Temporal variation of scintillation index: Overall response

The study is initiated with analysis of diurnal and seasonal behaviour of SI index (S_4) and their association with respective Rz, a few relevant outputs are presented in Figure. 4 separately for High Solar Active year (HSA) and Low Solar Active (LSA) periods. A class of seasonal pattern is revealed in the HSA period when the equinoctial months favor scintillation to grow, but in the LSA period, no strong seasonal pattern in scintillation is observed with low P.C.of occurrences in all the seasons compared to the HSA period, suggesting a strong role of solar activity to the .growth of a scintillation. However, the month-to-month changes in S4 with respective Rz status show no such influence (Figure. 4) even in HSA seasons. The shades of different types represent scintillation Occurrence P.C. in post-midnight, pre-noon, post noon and post-sunset hour.

Coming to the diurnal SI P.C occurrences features as displayed in Figure 5, separately for Equinoctial and Summer seasons and for the HSA and LSA status, one can see that as the day advances especially after sunset, the scintillation events during equinoctial months show exponential growth (Figure. 5a) during

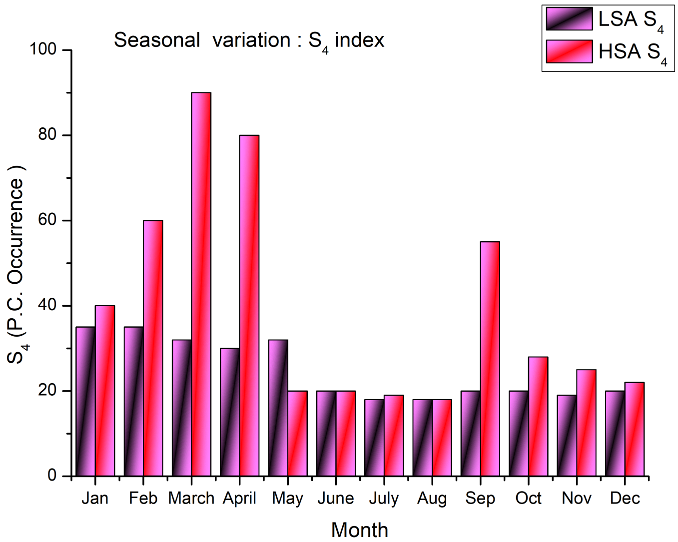

Figure 4: Displays seasonal variation of Scintillation Index S_4 ($1.2GHz$ in P.C)., in High Solar Activity (HSA) and Low Solar Activity LSA status where one can see that equinox month, favors scintillation to grow exponentially in the HSA period. In the LSA background, a significant decrease in scintillation activity is apparent. No strong seasonal preference for the growth of scintillation is observed in the LSA period.

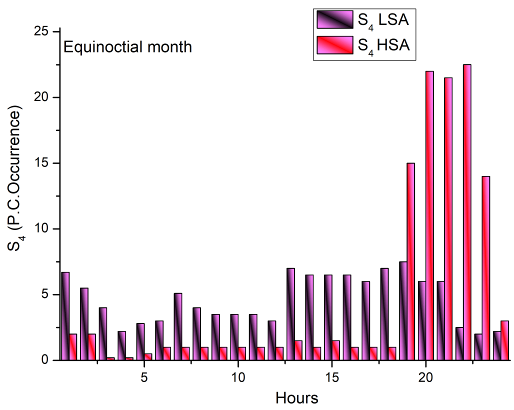

(a)

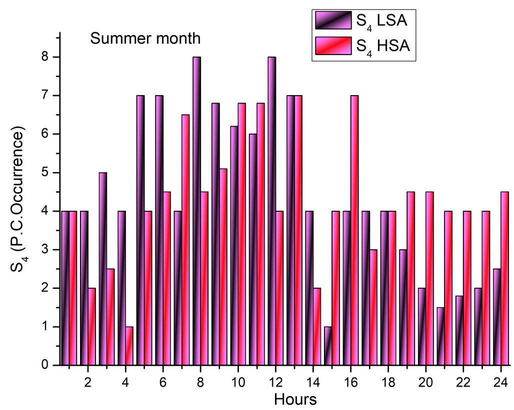

(b)

Figure 5: Diurnal variations of P.C. occurrence of S4 P.C (a) Equinoctial and (b) Summer season for both HSA and LSA status.

HSA period, though an increase in daytime Scintillation activity is noted during the LSA period compared to that of HSA. But in the summer there is no preferential time of spectacular increase in scintillation activity over the period as in equinoctial months but a marginal increase in daytime scintillation in the LSA period is also observed (Figure. 5b). These observations suggest that the post-sunset equinoctial scintillation has the source of origin associated with the anomaly effect which will be our main interest of study here.

2.2 TEC profile features; Growth and Inhibition of Anomaly and Solar Role (in absence of GMS events) :

As our interest lies in Anomaly–scintillation associations, it is necessary to present relevant electron content profiles, especially of Equinoctial months when Anomaly is strong compared to solstices. As a comparison, two GPS-derived TEC profiles over Guwahati, one for an equinoctial month and the other for solstice are presented [Figure. 6] along with global TEC maps. In Figure. 6a(i), a vernal equinoctial GPS-derived TEC profile shows the growth of a secondary density peak in the late afternoon hours which is stronger than the local noon maximum, and then the decay starts where our study on scintillation is focussed. The development of the strong secondary peak is the Anomaly, also seen in the global TEC map of the equinoctial month of March 2011 [Figure. 6a(ii)]. On the contrary, the summer solstice shows a not-so-active formation of the anomaly as one can note from the 2009 June GPS-derived TEC profile [Figure. 6b(i)] and also in the TEC global map of the summer solstice of 2017 [Figure. 6b(ii)]. The 2017 year is chosen in absence of relevant global data for 2009 and there will be no solar discrepancies on TEC because both the years are of low solar status [Figure. 7]. No clean secondary or late afternoon maximum (low value of 35-40 TEC U) in TEC profiles at the hours suggests weak or absence of the equatorial anomaly during solstices.

In this connection, we also present the TEC global map of June 4, 2022, with Rz=66 to focus on that even with the increase of Rz status, there may not be a strong development anomaly during the solstice (Figure. 8).

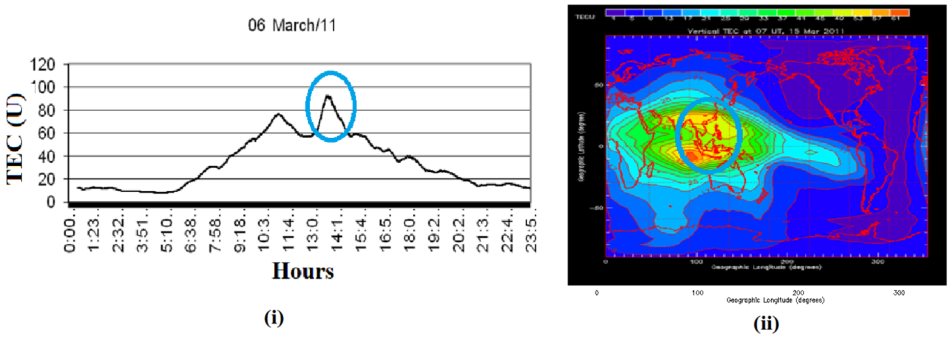

(a)

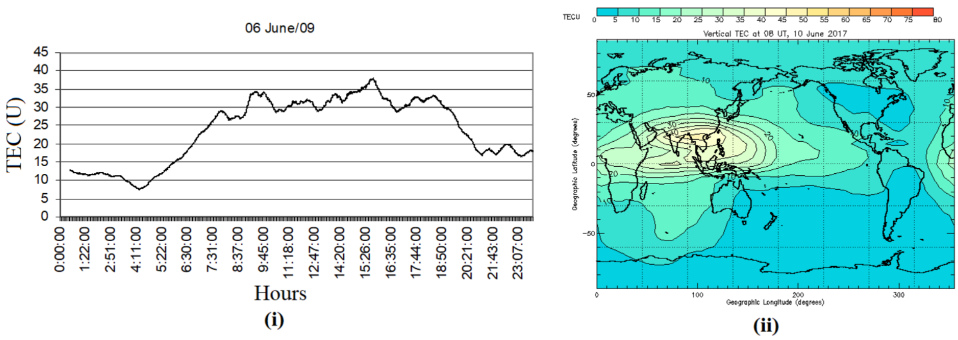

(b)

Figure 6: TEC profiles :(a) of the equinoctial month (i) GPS-derived and (ii) Global map, also note the development of anomaly signature (circled); (b) of the solstices (i) GPS-derived and (ii) Global map, no signature of the anomaly.

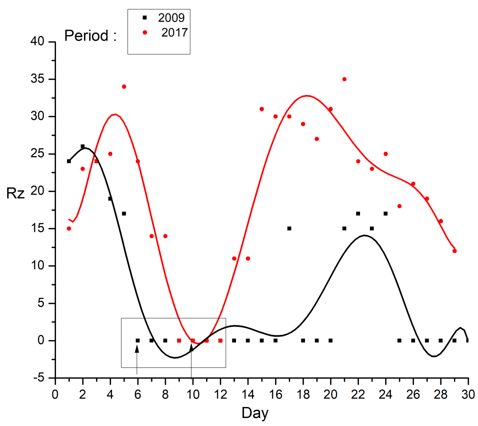

Figure 7: Rz diurnal variation in the month of June 2009 and 2017. The TEC profiles are compared at Rz minimum as marked

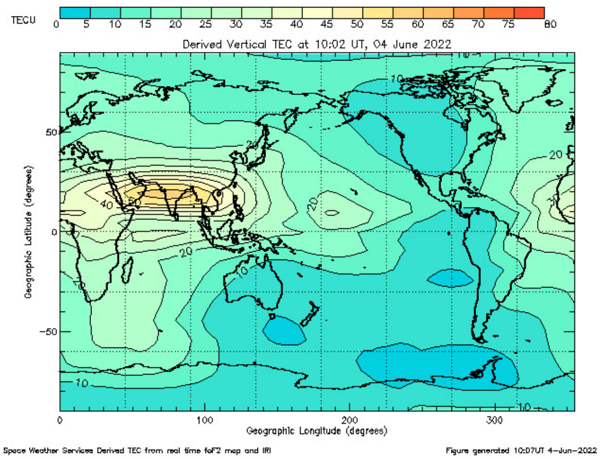

Figure 8: TEC Global map for a 2022 solstice period. It shows that even with the increase of Rz to 66, the anomaly strength does not increase as in equinoctial months.

2.3 TEC features, Scintillation and their association (in solar quiet condition)

Scintillation as we have seen is basically an equinoctial phenomenon with more events in post-sunset hours, contrary to solstice when daytime scintillation events are more in number. Our focus as has already been highlighted is on relevant sources associated with post-sunset equinoctial-type scintillation in differences mainly to that of solstices.
Scintillations are the product of the scattering of signals from small-scale irregularities, formed as a result of wave-wave interactions, breaking of density gradient when heavy fluid gets dumped over light fluid, dissipation of gravity waves as they move up from its origin (troposphere) to the ionosphere, to name a few. Therefore, the contributions of electron density and its gradient are essential aspects that need to be examined in association with the growth of scintillation as presented in the following articles.

2.3.1 Observations during Low Solar Active (LSA) periods

Equinoctial month :
In search of possible causes of scintillation during equinoctial months, we present a typical TEC profile of April 2009, an LSA period along with scintillation where Figure. 9a is the one constructed from all the satellites as it crosses the FOV of the receiver and Figure. 9b is the moving average profile, displaying a fast enhancement in density at local noon (1200 hrs), and another relatively low in magnitude at 1630 hours, thereby presenting an initial sharp decay at 1200 hrs and with a break in decay magnitude at 1800 hrs., TEC reaches back to its low at 2300 hrs.

Important features here are the (i) fast rise of density in the morning, (ii) fast decay after reaching a diurnal peak in the noon, and (iii) the post-sunset rise in TEC (though weak in magnitude) where we focus our interest.

Scintillation diurnal pattern on this day also reveals the presence of three peak activity periods((i) in the morning at 0500 hrs with the fast growth of TEC,(ii) at 1230-1300 hrs with fast decay after reaching its diurnal peak, and (iii) at 1830-1930 hrs with the decay of TEC after attaining the post-sunset secondary peak, though weak in magnitude.

Thus the relevance of TEC decay /growth on scintillation cannot be brushed aside and important feature to take note of.

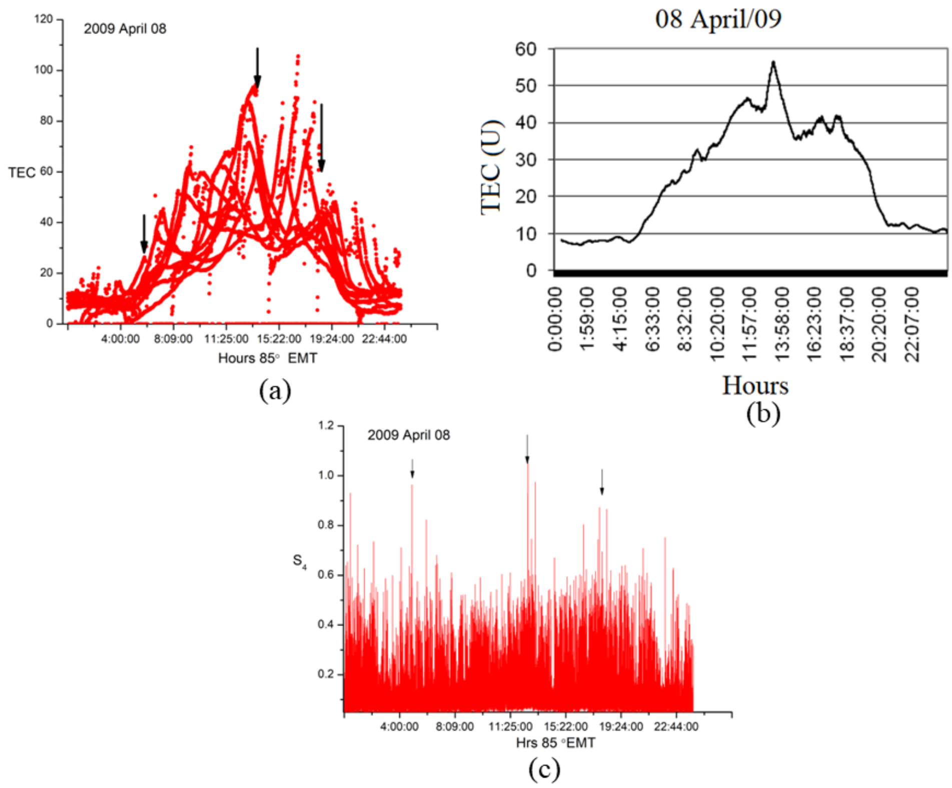

Figure 9: Displays an equinoctial (a)TEC profile from all satellite passes ; (b) Moving average plot and (c) Scintillation events on the day of April 2009. The modulation in scintillation is associated with fast growth and decay rate of TEC (marked by arrow)

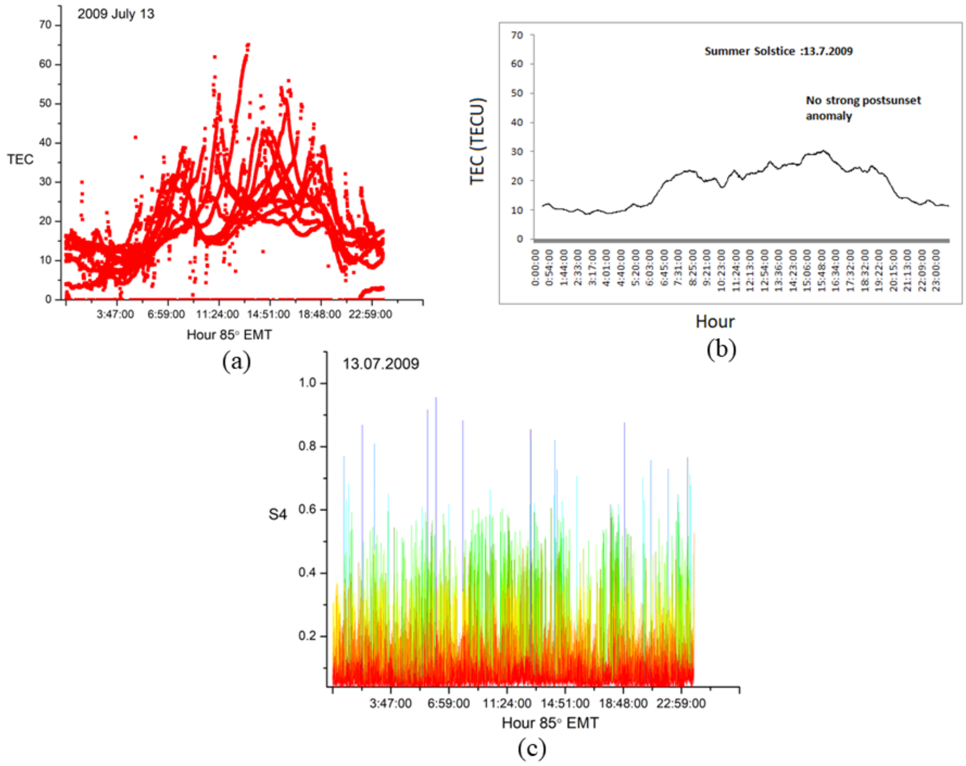

Figure 10: Displays solstice-time (a)TEC profile from all satellite passes;(b) Moving average plot and (c) Scintillation events on July 13, 2009. Note no strong post-sunset anomaly and no strong scintillation at this hour.

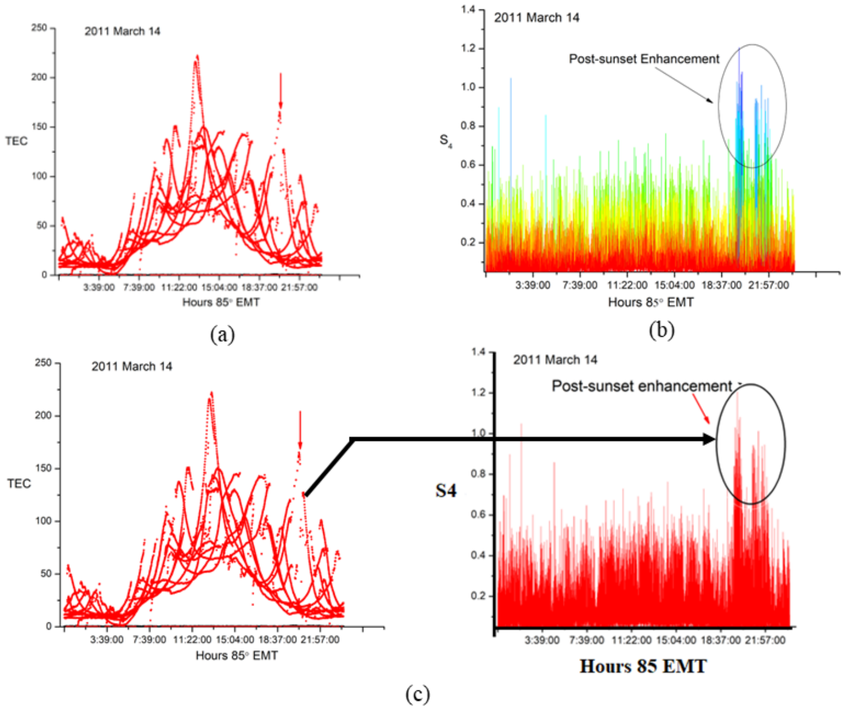

Figure 11: (a)TEC profile during sn equinoctial month ; (b) Scintillation index S4 in the relatively strong solar background and (c) Anomaly feature and scintillation. Note strong anomaly signature and strong scintillation at post-sunset hours.

Solstice season:

In Figure. 10, a representative LSA summer solstice TEC profile of July 2009 along with scintillation is presented. Here, Figure. 10a is the profiles constructed from all the satellites as it crosses the FOV of the receiver and Figure. 10b is the average TEC profile, displaying no clean post-noon peak but maintaining more or less constant density beyond sunset hours to decay gradually. The scintillation events of Figure. ?? also show no preferential time of occurrence and are present throughout the day (Figure. 10) more or less with the same intensity. Therefore important feature during LSA solstices is that the TEC profile does not show any preferential time of its growth, with no strong post-noon peak and the same goes with scintillation.

We now present the scintillation status during the High Solar Active (HSA) years.

2.3.2 Observations during HSA periods

Starting with the TEC profile features during this High solar Active period, Figure. 11a represents an equinoctial TEC profile (oblique mode) displaying a large accumulation of density at the post-sunset and beyond hours in a relatively strong solar background (Rz= 110). Important to note is the growth of sudden and severe scintillation almost in coincidence with the development of the strong anomaly during this period (Figure.11b,c).

In solstices, even with the enhancement of solar status, the TEC diurnal patterns neither show any large accumulation in the after-sunset ionization density (Figure. 12a) nor any preferential time of

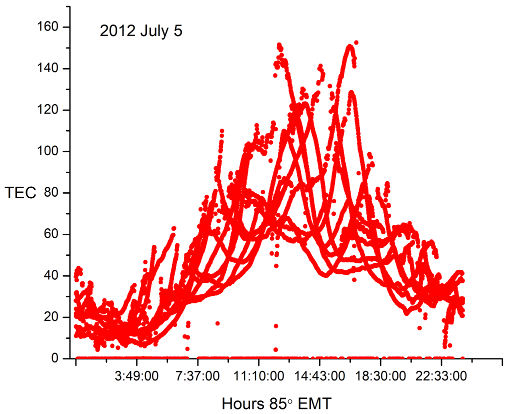

(a)

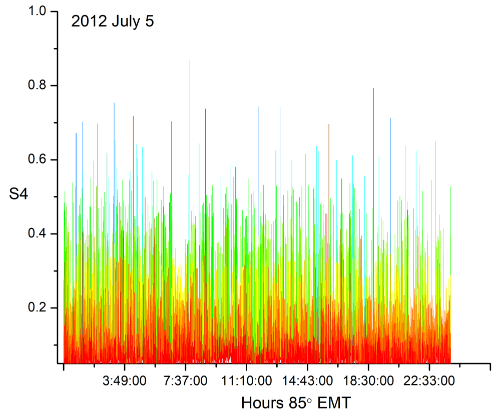

(b)

Figure 12: During solstices, even in the HSA period there is (b) neither a preferential time of occurrence of strong scintillation (a) nor the signature on the development of anomaly in the TEC profile.

enhancement of scintillation occurrences (Figure. 12b), the profile character more or less maintained the same as that of the LSA period but only with an increase in TEC peak value.

2.3.3 Analysis Output (Solar quiet background)

In LSA Period:

1. The equinoctial Scintillation diurnal pattern reveals its relatively strong occurrence during morning and afternoon features in association to the TEC decay /growth rate but post-sunset enhancement in TEC shows no significant contribution to scintillation, because of weak anomaly strength.
2. The Solstice scintillation displays no temporal preferences in occurrence features unlike in the equinoctial months and maintained a balanced feature from morning till late afternoon with a short time increase in scintillation strength similar to the diurnal TEC profile which maintains more or less constant density beyond sunset hours with no post sunset peak. Therefore important feature during LSA solstices is that the TEC profile does not show any preferential time of its growth, with no strong post-noon peak and the same goes with scintillation.

In HSA Period:

1. A strong accumulation of density occurs during Equnoctial post-sunset hours (1800 – 2000 hrs), along with an explosive enhancement in scintillation. This is the result of anomaly formation and dissipation after sunset hours.
2. But during solstices, even in the HSA period, there is (a) neither a preferential time of occurrence of strong scintillation (b) nor the signature on the development of anomaly in the TEC profile (Figure. 13).

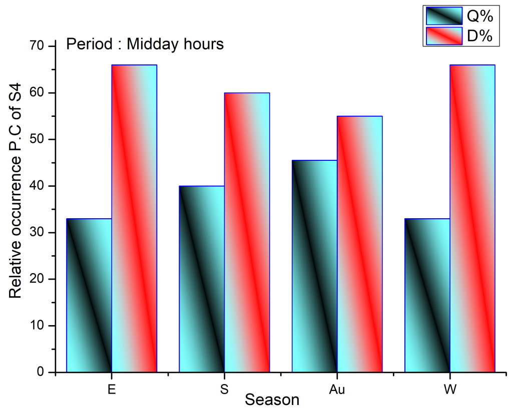

(a)

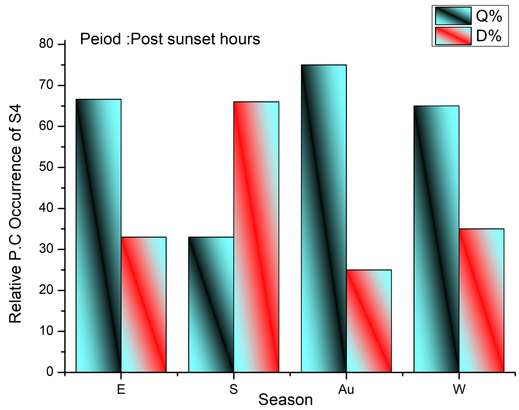

(b)

Figure 13: Relative occurrences of P.C of Scintillatin index S4 (a) Noon time and (b) Postsunset hours at different seasons and during quiet and disturbed environments.

Role in reception quality:

Thus, the process of growth of Equatorial anomaly especially during quiet days of the HSA period offers a strong contribution to the exponential growth of equinoctial post-sunset scintillation, though with little effect on both during solstices and LSA periods.

The resultant effect is the possible degradation in quality reception during equinoctial post-sunset hours of the HSA period.

2.4 Contribution of Geomagnetic factors to Scintillation

The situation during GMS is likely to be at variance with that of normal days because of the complex dynamics involved in the release of a magnetic storm, and this being the subject matter of the work here, we now introduce this aspect briefly and to present relevant analysis with the following issues as aims :

i. The GMS and the growth of the Anomaly.

ii. Resultant effect of GMS on GHz scintillation in the background of Equatorial Anomaly.

But, before analyzing scintillation in response to the GMS, we present in Figure 13 the relative occurrence of P.C occurrence of S4 during noon and post-sunset hours in relation to magnetic index Kp. The result is clear as overwhelm, the noon time scintillation shows association with Disturbed day environment wheres during post-sunset hours except for the summer solstice, the Quiet day scintillation dominates. Against this background, we will now open our analysis of scintillation with GMS events.

2.4.1 Magnetic storm time signal feature and Equatorial anomaly

Background: A geomagnetic storm is one of the major disturbances in earth's magnetosphere and its effect on the ionosphere is a well-studied area, yet there are a few aspects that still need to be addressed for possible framing of a reliable predictive model, especially with reference to scintillation related issues. Another important aspect to note is the growth of severe magnetic storms with respect to solar activity because such storms occur not at the solar peak but at moderate solar status. Therefore, anomaly events

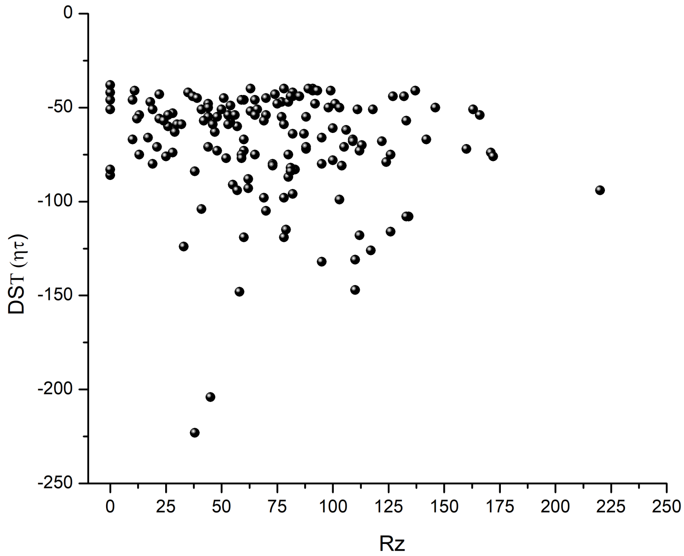

Figure 14: Mean DST and Rz (2008-2016) relation. Note that strong GMS events are likely to occur more within a specific Rz and are less likely to develop at the highest solar epoch.

when seem to intensify at strong solar backgrounds, the severe magnetic storms grow at the moderately active status of the sun as demonstrated in Figure. 14 during the period 2008 to 2016 covering strong to weakest solar staus. Therefore, in this exercise, we will analyze the role of GMS in terms of the respective strength to the development or inhibition of anomaly and the consequent contribution to the growth of scintillation, with a few case presentations.

2.4.2 Case presentation: TEC and Scintillation at different GMS events

Case 1: March 2015 Geomagnetic Storm

It is seen from the DST profile of this month (Figure. 15) that solar quiet-time behavior exists till the early hours of March 17, and then a storm commences with an SSC to reach the maximum depression in the early hours of March 18. The scintillation diurnal feature as expected during HSA post-sunset hours shows large enhancements on March 17 (Figures. 16c) along with strong post sunset Anomaly as displayed by individual satellites while crossing the FOV of the receiver (Figure. 16a) and also in the average TEC profile of the day Figure. 16b), but on the day of maximum depression (March 18), an absence of intense equinoctial postsunset scintillation (Figure. 16d) is to be noted also that the TEC profile shows a decrease in its value by 80% with no development of Post- Sunset anomaly (Figure. 16e,f).

Analysis output:

(i) During the main phase of the GMS, on March 18, the inhibition of the growth of anomaly along with the absence of post-sunset equinoctial scintillation is significant.

(ii) But on Mach 17(no storm day) strong scintillation event is present in association with the clear post-sunset anomaly, as expected.

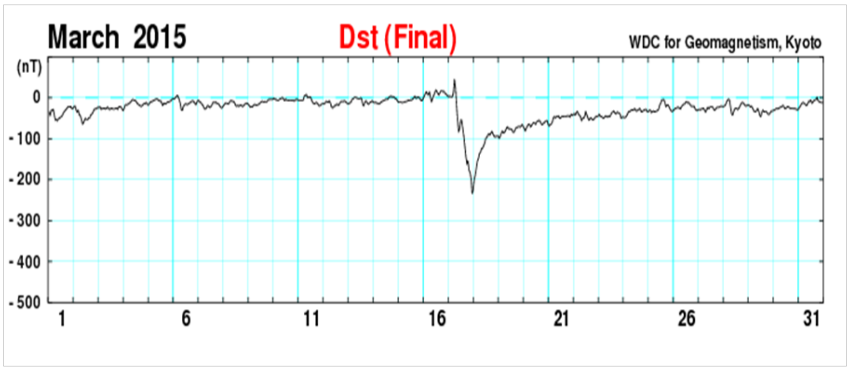

Figure 15: Mean DST and Rz (2008-2016) relation. Note that strong GMS events are likely to occur more within a specific Rz and are less likely to develop at the highest solar epoch.

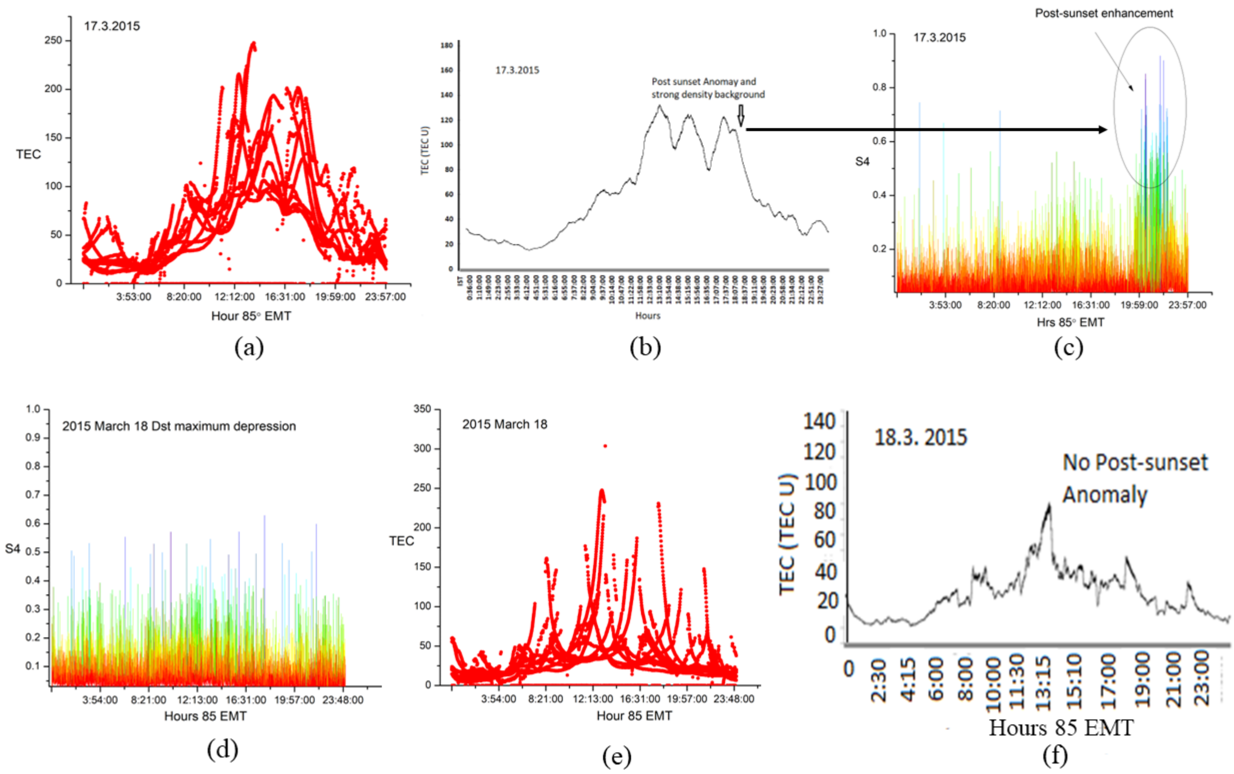

Figure 16: (a) TEC profiles of March 17, 2015, of all satellite Passes,(b) Average TEC profile on March 17, (c) Scintillation on 17 March (d) Scintillation on March 18, 2015 (e)TEC profiles of all satellite passes on March 18, and (f) Averaged filtered profile of March 18 (day of maximum depression).

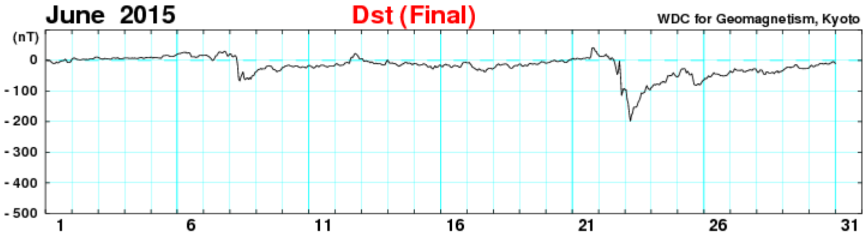

Figure 17: Dst profile of June 2015

(iii) Such events provide supporting inputs as to how the anomaly effect enhances density and how this aspect is related to the growth of scintillation.

This observational aspect will be brought into the discussion along with the results of case studies that are followed.

Case 2: June 2015 GMS event

The GMS started with an SSC on the early morning hours of 22.6.2015 (00:30 hrs) and reached maximum depression (-198 nT) on June 23 at 1130 hrs (IST or 85° EMT), the recovery was gradual to attain the normal level on March 30 (Figure. 17). The respective profiles of scintillation and TEC of June 22 presented in Figures. 18a and 18b show no GMS effect either in the Scintillation or in TEC by displaying the normal summer pattern with the absence of temporal enhancement in scintillation and of the postsunset anomaly. On the day of the main depression i.e on the 23rd of June (Figure. 18c, 18d), an anomaly was formed but with no contribution to scintillation either in magnitude or in frequency, likely due to relatively low background density, an issue we will bring into the discussion.

Analysis Output:

i. GMS effects on scintillation were not significant during this summer storm even on the maximum depression day.

ii. A weak post-sunset anomaly appeared on this day but storm-induced effects seem no effect on this process.

iii. Absence of an anomaly or a weak one and no post-sunet intense scintillation are the usual Solstice features and thus storm effects are not apparent.

Case 3: March 2016:GMS event

In this month a single GMS event occurred with an SSC on March 6 at 1630 (IST) hrs and maximum depression at 03:30 hrs on March 7 (-99 nT), the recovery was gradual, the low Dst value (-50 nT) even retained till 07:30 hrs of March 8 (Figure. 19).
The scintillation diurnal pattern on March 6 shows inhibition of normally present strong post-sunset scintillation (Figure. 20a) and TEC record from individual satellites passing through FOV (Figure. 20b) as well as filtered TEC profiles (Figure. 20c), show an anomaly but the peak is not strong compared to the daytime maximum.

On March 7, the day of maximum depression in Dst, a relatively strong scintillation though short-lived was detected after sunset hours (Figure. 21a). Looking into the TEC profiles both from individual satellite records (Figure. 21b and filtered ones Figure. 21c), a relatively strong anomaly peak higher than

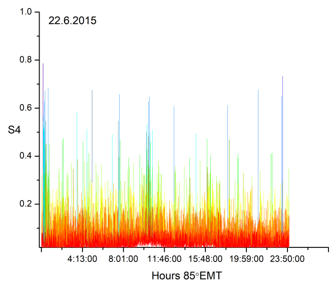

(a)

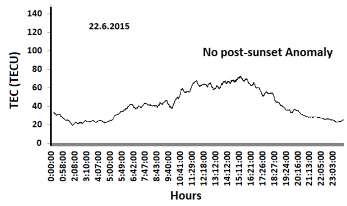

(b)

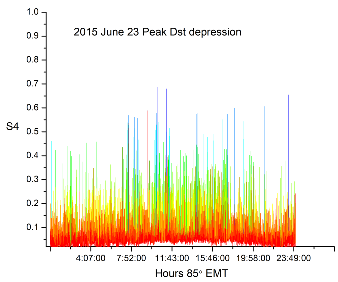

(c)

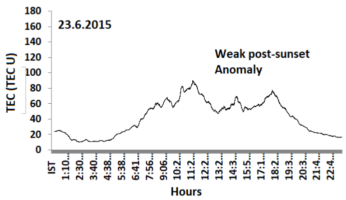

(d)

Figure 18: (a) Scintillation June 22 and (b) TEC profile of June 22; (c) Scintillation of June 23 (day of maximum Dst depression) (d) TEC profile of June 23. No GMS effect is reflected in the Scintillation profile either in magnitude or in the temporal pattern.

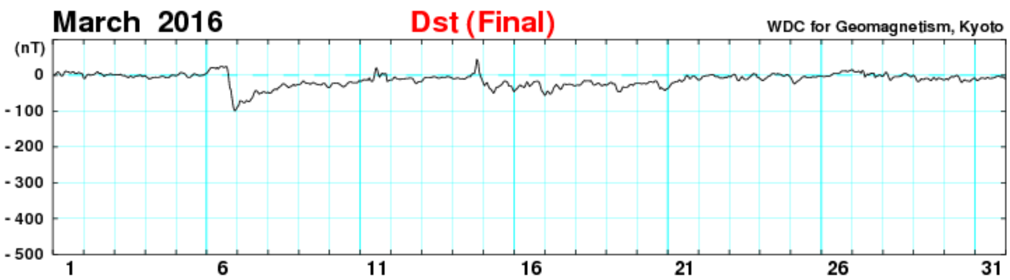

Figure 19: Dst profile of March 2016

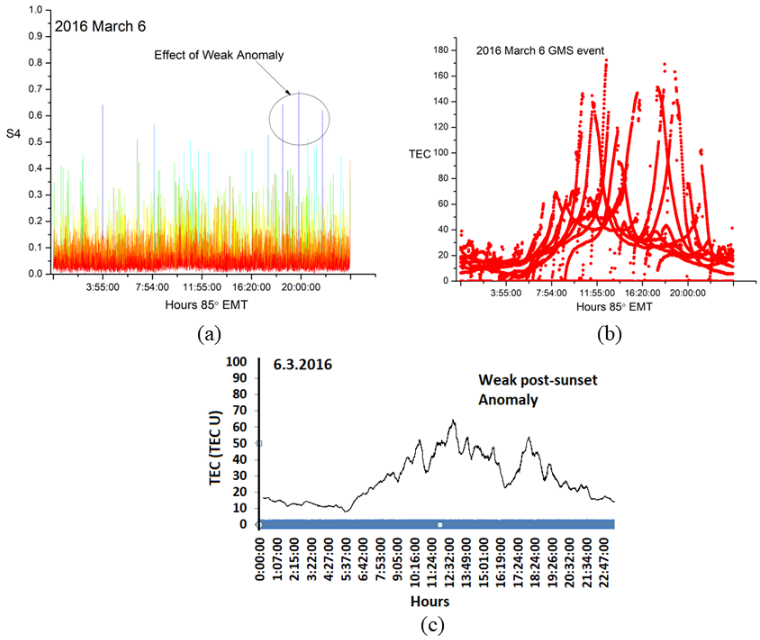

Figure 20: (a) Scintillation diurnal pattern on March 6, 2016, with weak anomaly effect ;(b) TEC record from all individual satellites passing through FOV of the receiver and (c) Filtered TEC profiles, note the presence of weak anomaly signature.

the daytime maximum was observed at 1730 hrs, almost in coincidence with the scintillation growth time. But the short-lived nature of scintillation which is in no comparison to normally present intense hour-long post-sunset equinoctial scintillation is likely due to the low TEC peak background, for sustaining the instability a parameter of importance in this aspect which we will refer again.

Summary of the overall observations:

(i) **No Strom Day**

(a) The analysis presents the role of equatorial Anomaly in the growth process of scintillation, especially seen during HSA post-sunset hours of equinoctial months when intense scintillation may lead to disruption in the communication link.

(b) In solstices, the situation is not acute, and anomaly even forms, because of the weak background density strength, the post-sunset scintillation is not triggered even in HSA periods.And communication quality is not likely to suffer.

(ii) **During GMS events**

(a) With the selected representative cases, it is clear that during solstices, there is no modification of scintillation either in temporal feature or in strength, and even if an anomaly forms but of weak background density, the effect of GMS is not significant to disturb communication mode.

(b) Also, the inhibition of scintillation during the maximum depression day of the equinoctial HSA period suggests improvement of signal quality on such strong GMS events when in normal situations the post-sunset severe scintillations are likely to degrade reception quality.

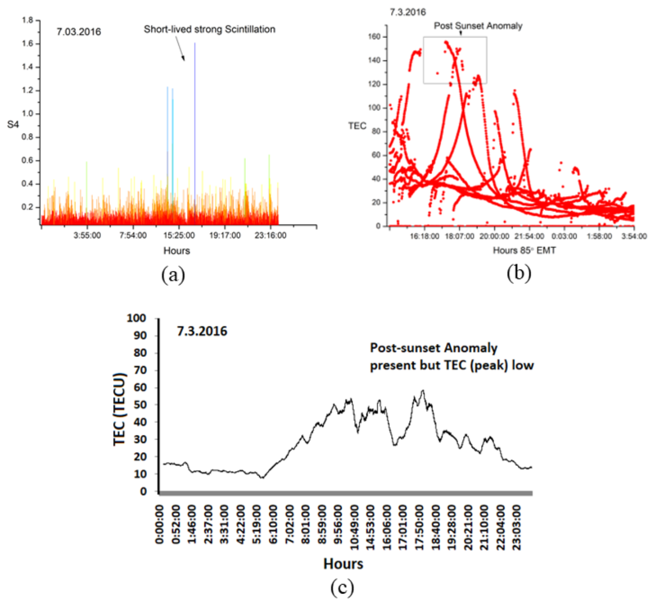

Figure 21: (a) Scintillation on March 7, 2016, (b) TEC record from all individual satellites passing through FOV of the receiver, and (c) Filtered TEC profiles. Short-lived strong scintillation in synchronization with the post-sunset anomaly and in the background of low TEC_{peak} compared to normal Q-day status.

However, even if strong scintillation develops on the maximum depression day of the equinoctial month, communication is not likely to suffer because of the short-lived nature of these events.

(c) In short, it is observed that anomaly is inhibited or decreases its strength in severe storm conditions during the main phase of the equinoctial season resulting in the inhibition of intense scintillation normally developed during post-sunset hours, thereby improving signal quality. In solstice, no storm-induced growth of scintillation is observed to disrupt communication links even during severe storm environments.

3 Discussion

The postsunset occurrence of scintillation at the equatorial and low latitudes is not a new finding. There are relevant theories proposed through observations, and model computation to understand the sources of scintillations [Aarons, 1982; Aarons et al., 1981; Wernik and Liu, 1974]. Sources of the postsunset anomaly are attributed to the bottom side F region irregularities generated by collisional shear instabilities, post-sunset vortex, and gravity waves [Hysell et al., 2017, 2014; Kudeki et al., 2007; Lund and Fritts, 2012] to name a few.

In the GMS environment, the situation is more complex, especially at the anomaly crest station [Devi et al., 1996a,b, 2002; Ogawa et al., 1980], and as the subject matter here especially on Geo-Magnetic Storm (GMS)-related scintillation and anomaly, we bring here a brief discussion relevant to geomagnetic storm-induced effects on the atmosphere of different strata. However, it is not the scope of the paper to elaborate on the complex process that triggers GMS, and will only bring the aspects relevant to the study and the observational results.

In brief, during a magnetic storm, a strong eruption of highly magnetized particles from the sun caused a Coronal Mass Ejection (CME) and generates disturbances in the earth-magnetosphere through the energy exchange processes from the solar wind (in plasma state). This results in transporting plasma from the neutral sheet of the magnetosphere toward the night side of Earth thereby bringing a modification in the ionospheric system. One of the sources generally associated with such changes is storm time Electric field when the shielding layer in the magnetosphere becomes ineffective and allows electric fields to penetrate directly to low latitudes [Fejer et al., 1999], this dynamo electric field is westward during daytime and thus may manifest itself like EXB drift, initiating charge movement from higher to lower latitudes, decreasing density at high latitudes and modify the same (may increase /decrease) at lower latitudes depending on the field strength as well as on the latitudinal locations. Abdu [1997]; Basu et al. [2007]; Carter et al. [2016]; Devi et al. [2018]; Fejer et al. [1979]; Fejer and Scherliess [1995] have observed through comparative analysis of the magnetic storm-induced effects on the ionosphere for a few events of weak to very strong intensity, covering periods from 2011 to 2015 by utilizing foF2 data collected at high/mid-latitude station of IZMIRAN (55.47° N, 37.30° E, $\Phi = +50.82\circ$) and mid-latitude station Alma-Ata (43.25°N, 76.92° E, $\Phi = +33.42°$) and Total Electron Content (TEC) profiles of Guwahati (26.148° N, 91.73° E, $\Phi = +12.30°$), an equatorial anomaly crest station, that during severe storms Guwahati experiences large depletion in TEC magnitude similar to high-mid latitude stations. This large TEC depletion at the anomaly crest station during a strong GMS event is explained through the development of an effective west ward storm-time electric field that may be strong enough to inhibit /slow down the growth process of an equatorial anomaly, especially during equinoctial months, resulting to reduction of the flow of plasma from the equator to off equatorial stations. Thus during severe GMS events, a negative ionospheric effect may be attained at anomaly crest stations as observed in Guwahati, especially during equinoctial, months.

Abdu et al. [2012] reported modification of equatorial anomaly modification under storm-time electric fields when a storm-time PPE (Prompt Penetration of Electric Field) may cause the crest of the anomaly to expand even up to mid-latitude resulting in a large increase in the daytime TEC and expansion of the anomaly to mid-latitude. Similar observations and conclusions are also drawn by Zhao et al. [2005]. The behaviour of GPS ionospheric scintillation during a strong magnetic storm was studied near the magnetic equator at Vanimo station and the storm-induced enhancement of scintillation was described due to the prompt penetration of eastward electric field in association with the southward turning of the IMF and intensification of AE that lifts the ionospheric plasma to certain height through the E × B mechanism. But in Guwahati, unlike their results, a strong decrease in density is observed in the severe magnetic storms [Devi et al., 2018] and also in the present case studies.

However, the situation is made complex with the disturbed time meridional neutral wind by lifting of ionospheric plasma along geomagnetic field lines to regions of lower loss rates, thereby enhancing the magnitude of density even at high latitudes resulting in positive ionospheric effect at low latitudes. The presence of positive and negative modulations in density at mid and low-latitude stations is also contributed by storm-time changes in neutral composition density.Thus, the combined roles of, magnetic field, meridional wind, and composition changes during severe storms along with the effective westward electric field result in the inhibition or growth process of an equatorial anomaly.

We present here aGlobal TEC profiles (Figures. 20) when Anomaly is inhibited by the storm-induced dynamics. In the equinoctial GMS event of March 18, 2015 (Figure. 22a) when on no-storm days strong anomaly dominates the entire anomaly belt, the inhibition of the same during the main phase is clear and significant (Figure. 22b).

Coming to the scintillation phenomenon, the situation varies with latitude .longitttude, and observation period. There are also reports of an increase in scintillation during a severe storm over the GHz range [Ogawa et al., 1980], unlike our observation. The latitudinal effect is important here. In low latitude

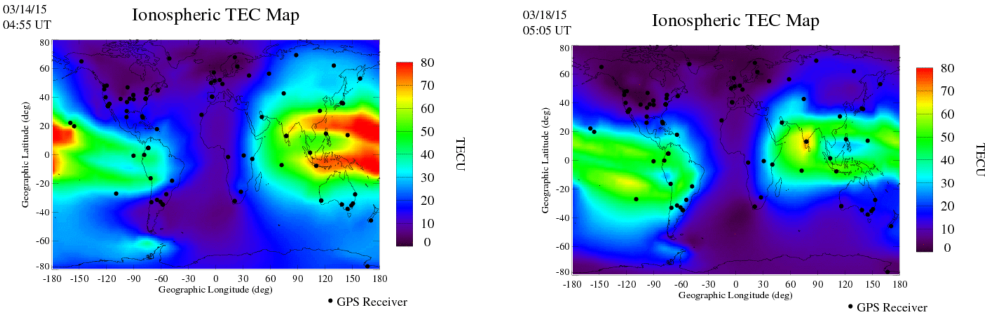

(a) (b)

Figure 22: (a) presence of Anomaly before March 18 2015 GMS (b) absence of the same during the main phase.

zone especially in post-sunset cases, the equatorial electric field plays a significant role. Because of the reversal of the daytime eastward field after sunset when a large increase in E field occurs that (prereversal enhancement) pushes the plasma up from the equator to low latitude to form a strong post-sunset density peak. The larger the magnitude of the electric field, the more is pumping force, and thus steep will be the decay rate once the phenomenon stops. The sharp decay when the atmospheric system is top heavier causes Rayliey Taylor instability and the process attributes to the generation of small-scale structures. The size of the irregularities of dimension (comparable to the wavelength, $\lambda \leq 1cm$) results in scattering and the scintillation process grows. Thus we see that in the following background conditions the scintillation grows with the active process of the anomaly: (i) Higher background TEC (> 80 suitable) (ii) Anomaly peak stronger than noontime peak (preferable) (iii) fluctuation greater than 30/40 TEC unit from the normal decay.

We see that in most of the strong GMS cases and during the main phase, the anomaly is inhabited because of density depletion or negative ionospheric effect, and in the absence of the necessary background conditions the anomaly could not develop, and signal degradation is less affected except for a few short-lived strong S4 magnitude.

Also, there are events though rare, when in presence of well-developed anomaly and strong density background, intense scintillation may not .grow.As an example, we take the March 2012 GMS event, which started on March 8 with an SC and maximum depression occurred on March 9 at 1400 hrs, (Figure. 23). We present the Dst profile along with TEC on March 9 (also with accompanied scintillation. But even in the presence of a well-developed post-sunset anomaly, in the strong TEC max background, the scintillation profile shows no intense feature during post-sunset hours.

A case of difference sun-set hours and unlike the strong negative effect on the main phase, the TEC retained the quiet day feature, but except for an early morning relatively isolated but strong event (though before the main phase) scintillation profiles do not reflect storm-induced effect. Searching for the sources of its origin we note that this particular scintillation is caused by a satellite with PAN-2, which appeared in the FOV of the receiver from location 85° E and latitude 10° N at an elevation of 5.5°.i.e., from a low elevation angle. Such situations in oblique mode (as in this case) has likely of tropospheric origin because during GMS background atmospheric modifications are also reported [Danilov and Lastovicka, 2001] and tropospheric modification is expected through the Forbush effect [Devi et al., 2018] when the temperature may increase or decrease resulting in a modification in RRI and effective earth radius factor. Thus, satellites that are not generally within the FOV of the receiver may appear in such an environment and cause scintillation through multipath scattering processes. However, such situations

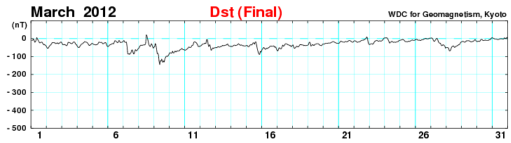

(a)

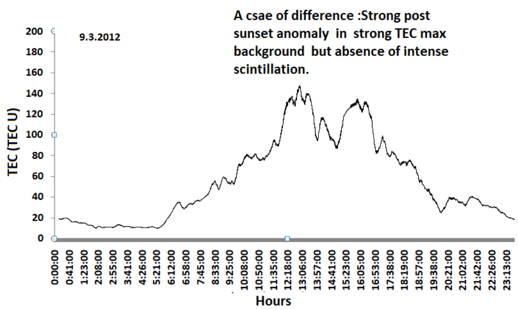

(b)

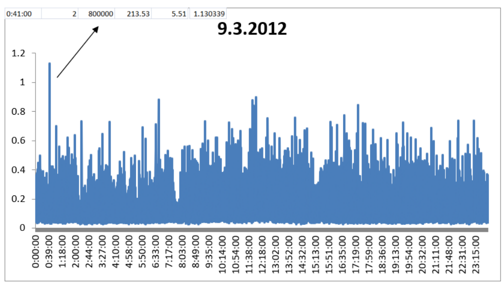

(c)

Figure 23: (a) presence of Anomaly before March 18 2015 GMS (b) absence of the same during the main phase.

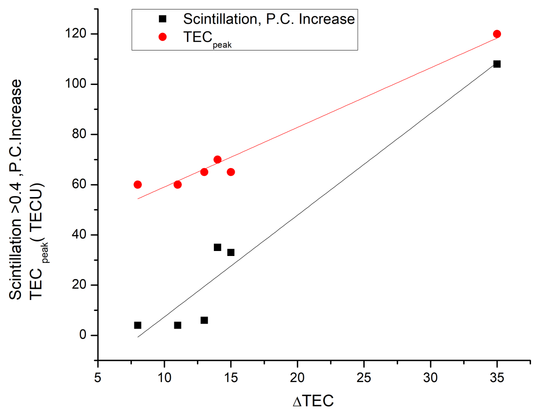

Figure 24: S4 P.C increase from the average with, TEC_{peak}(bacgrund) and $\Delta TEC/hr$

are generally avoided when observations are confined to the vertical mode of reception only. But the point of significance is that the tropospheric origin of the scintillation during a geomagnetically disturbed environment may also disrupt communication, an area that needs special review and will be our plan of work for the future.

Finally, the resultant storm-induced modification in density is dependent on the effect of both the electric fields one pushing plasma up from the equator and the other carrying plasma down from high latitude, resulting to positive /negative effects with different intensities at low /anomaly crest station based on strength of eastward/westward fields which vary with storm magnitudes as well as occurrence time and season of the storm. And stronger the anomaly the sharper would be the decay rate and the more effective will be instability processes to grow and hence scintillation. Thus electron density fluctuation from the background level is one of the key parameters in this regard.

Wernik and Liu [1974] decades back observed that an irregularity slab of the order of 200 km with electron density fluctuation of about 20 percent from the background is likely a candidate for the observed maximum S4 values. Aarons et al., [1981] also reported similar results while analyzing equatorial and anomaly zone scintillation levels at 1.5 GHz .that the post-sunset period density fluctuations over anomaly crest are proportional to the scintillation. We see here in this aspect that the necessary conditions for intense scintillation to grow are fluctuations from background TEC that should be more than 20 units and in a background of high TEC_{peak} environment ($> 75TECU$) to satisfy the instability to grow. We calculate TEC fluctuation magnitude from the average background (ΔTEC) and the TEC_{peak}(at the decay point) and the P.C increase of Scintillation events $S_4 > 0.4$ during the post-sunset period, (Figure 22) and observe that TECpeak and fluctuations provide coupled influences in generating irregularities because higher the density, the decay is the faster suitable for creating a dynamical situation leading to Rayle Taylor instability associated with producing small scale structures triggering scintillation. Thus negative storm effect during severe storms over Guuuwhati results in the absence of anomaly, reducing background density with no enhancement of POST sunset density to generate a strong decay rate for triggering instabilities and scintillation. Thus Anomaly has a strong role especially in post-sunset scintillation with exponential enhancement during a quiet time and inhibition of the same during severe GMS events and the consequent contributions of scintillations to signal reception quality are likely a deterioration during no-storm days and improvements of the same during GMS events.

4 Conclusion

The paper that aims in understanding the role of Equatorial Anomaly in the reception quality of a signal by analyzing parameters mainly $1.2GHz$ scintillations over the Anomaly crest (26°N,92°E 15° N Geomagnetic latitude) station, offered the results of quiet day as well as during GMS environments.

The scintillation growth is associated with TEC fluctuation magnitude from the background, and TEC peak value (at the time of decay), especially in the post-sunset anomaly periods With TEC fluctuations of $>$ 20 units from the background and TEC peak density of $>$ 60 TECU , S_4 P.C occurrence may reach more than 60% and observe that TEC background and fluctuations (during the post-sunset scintillation time) provide coupled influences as higher the density, the background decay is faster and important dynamics for creation like Rayle Taylor instability sources associated with producing small scale structures triggering scintillation. We see here that fluctuations are from background TEC should be more than 20 units but also necessary to maintain a high TEC environment to satisfy the instability to grow with the increase of decay rate during strong GMS background.

Thus the combined roles of, magnetic field, meridional wind, and composition changes during severe storms along with the effective westward electric field result in inhibition or growth process of an equatorial anomaly, and in such situations density at anomaly crest stations like Guwahati especially during equinoctial months when anomaly plays a strong role in enhancing daytime electron content may show a decrease informer case and may enhance in the latter, but the inhibition is more often seen during string GMS event, thereby in the growth of scintillation. The strong role of the Anomaly, especially on quiet days of the HSA period, in the exponential growth of post-sunset equinoctial scintillation may lead to disruption in the communication link. In solstices, the situation is not acute, and anomaly even forms, because of the weak background density strength, the post-sunset scintillation is not generated in HSA periods.

In Solstice GMS events, no storm effect on the development of a strong post-sunset Anomaly was detected even in the HSA period and so there is no modification in scintillation either in temporal feature or in strength, and even if an anomaly forms but of weak background density, the effect of GMS is not significant either to disturb or improve communication mode.

In Equnoctial GMS events, the decrease in the strength of normally existing strong post-sunset anomaly especially during the main phase inhibits the growth process of usually observed intense scintillation at these hours, thereby contributing to improving signal reception quality.

Thus Anomaly has a strong role especially in post-sunset scintillation with exponential enhancement during a quiet time and inhibition of the same during severe GMS events and the consequent contributions of scintillations to signal reception quality that are likely a deterioration during no-storm days and improvements of the same during GMS events.

Quantitative work in this direction is the plan for the future.

References

Aarons, J. (1982). Global morphology of ionospheric scintillations. *Proceedings of the IEEE*, 70(4):360–378.

Aarons, J., Whitney, H. E., MacKenzie, E., and Basu, S. (1981). Microwave equatorial scintillation intensity during solar maximum. *Radio Science*, 16(05):939–945.

Abdu, M. (1997). Major phenomena of the equatorial ionosphere-thermosphere system under disturbed conditions. *Journal of Atmospheric and Solar-Terrestrial Physics*, 59(13):1505–1519.

Abdu, M., Batista, I., Bertoni, F., Reinisch, B., Kherani, E., and Sobral, J. (2012). Equatorial ionosphere responses to two magnetic storms of moderate intensity from conjugate point observations in brazil. *Journal of Geophysical Research: Space Physics*, 117(A5).

Appleton, E. V. (1954). The anomalous equatorial belt in the f2-layer. *Journal of Atmospheric and terrestrial Physics*, 5(1-6):348–351.

Barman, M., Devi, M., and Barbara, A. (1993). Scintillation observation over guwahati and computation with existing model. *Indian Journal of Physics*, 67:385–394.

Barman, M., Devi, M., and Barbara, A. (2000). Modelling on irregularities through correlated analysis of vhf scintillation and upper atmospheric phenomena. In *Proceedings of WOCEB-2k*, pages 73–77, Guwahati.

Basu, S., Basu, S., Rich, F., Groves, K., MacKenzie, E., Coker, C., Sahai, Y., Fagundes, P., and Becker-Guedes, F. (2007). Response of the equatorial ionosphere at dusk to penetration electric fields during intense magnetic storms. *Journal of Geophysical Research: Space Physics*, 112(A8).

Briggs, B. and Parkin, I. (1963). On the variation of radio star and satellite scintillations with zenith angle. *Journal of Atmospheric and Terrestrial Physics*, 25(6):339–366.

Carter, B., Yizengaw, E., Pradipta, R., Retterer, J., Groves, K., Valladares, C., Caton, R., Bridgwood, C., Norman, R., and Zhang, K. (2016). Global equatorial plasma bubble occurrence during the 2015 st. patrick's day storm. *Journal of Geophysical Research: Space Physics*, 121(1):894–905.

Danilov, A. and Lastovicka, J. (2001). Effects of geomagnetic storms on the ionosphere and atmosphere. *International Journal of geomagnetism and aeronomy*, 2(3):209–224.

Devi, M., Barbara, A., and Barman, M. (1996a). Ionospheric irregularities and storm-induced equatorial and high-latitude effects at the anomaly crest region. *Radiophysics and quantum electronics*, 39:179–187.

Devi, M., Barbara, A., and H, M. (1996b). Ionospheric disturbance and magnetic storm : A few case studies over tokyo and guwahati. In *Proceeding of SGESS*, Japan.

Devi, M., Barman, M., and Barbara, A. (2002). Identification of quiet and disturbed days through iec profile features over anomaly crest region. *Journal of atmospheric and solar-terrestrial physics*, 64(12-14):1413–1423.

Devi, M., Patgiri, S., Barbara, A., Gordiyenko, G., Depueva, A., Depuev, V., and Ruzhin, Y. Y. (2018). Storm time ionospheric-tropospheric dynamics: A study through ionospheric and lower atmospheric variability features of high/mid and low latitudes. *Geomagnetism and Aeronomy*, 58:857–870.

Fejer, B. G., Gonzales, C., Farley, D., Kelley, M., and Woodman, R. (1979). Equatorial electric fields during magnetically disturbed conditions 1. the effect of the interplanetary magnetic field. *Journal of Geophysical Research: Space Physics*, 84(A10):5797–5802.

Fejer, B. G. and Scherliess, L. (1995). Time dependent response of equatorial ionospheric electric fields to magnetospheric disturbances. *Geophysical Research Letters*, 22(7):851–854.

Fejer, B. G., Scherliess, L., and de Paula, E. R. (1999). Effects of the vertical plasma drift velocity on the generation and evolution of equatorial spread f. *Journal of Geophysical Research: Space Physics*, 104(A9):19859–19869.

Hysell, D., Fritts, D., Laughman, B., and Chau, J. (2017). Gravity wave-induced ionospheric irregularities in the postsunset equatorial valley region. *Journal of Geophysical Research: Space Physics*, 122(11):11–579.

Hysell, D., Jafari, R., Fritts, D., and Laughman, B. (2014). Gravity wave effects on postsunset equatorial f region stability. *Journal of Geophysical Research: Space Physics*, 119(7):5847–5860.

Kudeki, E., Akgiray, A., Milla, M., Chau, J. L., and Hysell, D. L. (2007). Equatorial spread-f initiation: Post-sunset vortex, thermospheric winds, gravity waves. *Journal of Atmospheric and Solar-Terrestrial Physics*, 69(17-18):2416–2427.

Lund, T. and Fritts, D. (2012). Gravity wave breaking and turbulence generation in the thermosphere. *J. Geophys. Res*, 117(10.1029).

Ogawa, T., Sinno, K., Fujita, M., and Awaka, J. (1980). Severe disturbances of vhf and ghz waves from geostationary satellites during a magnetic storm. *Journal of Atmospheric and Terrestrial Physics*, 42(7):637–644.

Wernik, A. and Liu, C. (1974). Ionospheric irregularities causing scintillation of ghz frequency radio signals. *Journal of Atmospheric and Terrestrial Physics*, 36(5):871–879.

Whitney, H. E. (1974). *Notes on the relationship of scintillation index to probability distributions and their uses for system design*, volume 74. United States Air Force, Air Force Systems Command, Air Force Cambridge ....

Zhao, B., Wan, W., and Liu, L. (2005). Responses of equatorial anomaly to the october-november 2003 superstorms. In *Annales Geophysicae*, volume 23, pages 693–706. Copernicus Publications Göttingen, Germany.